Exp Brain Res (2015) 233:1907–1919
DOI 10.1007/s00221-015-4262-4

RESEARCH ARTICLE

# Intermuscular coherence contributions in synergistic muscles during pedaling

**Cristiano De Marchis[1] · Giacomo Severini[2] · Anna Margherita Castronovo[3] · Maurizio Schmid[1] · Silvia Conforto[1]**

Received: 20 November 2014 / Accepted: 18 March 2015 / Published online: 28 March 2015


**Abstract** The execution of rhythmical motor tasks requires the control of multiple skeletal muscles by the Central Nervous System (CNS), and the neural mechanisms according to which the CNS manages their coordination are not completely clear yet. In this study, we analyze the distribution of the neural drive shared across muscles that work synergistically during the execution of a free pedaling task. Electromyographic (EMG) activity was recorded from eight lower limb muscles of eleven healthy untrained participants during an unconstrained pedaling exercise. The coordinated activity of the lower limb muscles was described within the framework of muscle synergies, extracted through the application of nonnegative matrix factorization. Intermuscular synchronization was assessed by calculating intermuscular coherence between pairs of EMG signals from co-active, both synergistic and non-synergistic muscles within their periods of co-activation. The spatiotemporal structure of muscle coordination during pedaling was well represented by four muscle synergies for all the subjects. Significant coherence values within the gamma band (30–60 Hz) were identified only for one out of the four extracted muscle synergies. This synergy is mainly composed of the activity of knee extensor muscles, and its function is related to the power production and crank propelling during the pedaling cycle. In addition, a significant coherence peak was found in the lower frequencies for the GAM/SOL muscle pair, possibly related to the ankle stabilizing function of these two muscles during the pedaling task. No synchronization was found either for the other extracted muscle synergies or for pairs of co-active but non-synergistic muscles. The obtained results seem to suggest the presence of intermuscular synchronization only when a functional force production is required, with the observed gamma band contribution possibly reflecting a cortical drive to synergistic muscles during pedaling.

**Keywords** Muscle synergies · Intermuscular coherence · Synchronization · Cycling · Neuromechanics · Surface electromyography

✉ Cristiano De Marchis
cristiano.demarchis@uniroma3.it

Giacomo Severini
gseverini@partners.org

Anna Margherita Castronovo
margherita.castronovo@bccn.uni-goettingen.de

Maurizio Schmid
maurizio.schmid@uniroma3.it

Silvia Conforto
silvia.conforto@uniroma3.it

[1] Biomedical Engineering Laboratory, Department of Engineering, Roma TRE University, Via Vito Volterra 62, 00146 Rome, Italy

[2] Department of Physical Medicine and Rehabilitation, Spaulding Rehabilitation Hospital, Harvard Medical School, Boston, MA 02114, USA

[3] Department of Neurorehabilitation Engineering, Bernstein Focus Neurotechnology, Bernstein Center for Computational Neuroscience, Georg-August University Göttingen, Universitätsmedizin Göttingen, Göttingen, Germany

## Introduction

Humans have a remarkable ability to integrate the activity of different physiological structures in order to perform movements of varying complexity. In particular, the coordination of cortical, supra-spinal and spinal circuits is key in performing fundamental highly repetitive tasks such as walking or cycling. These tasks are assumed to be

controlled by three main processes: cortical contributions related to voluntary command and high-level control, control of rhythmical activation by the spinal motorneurons through the central pattern generators (CPGs), and online reflex-driven adjustments (Ivanenko et al. 2005; Petersen et al. 2012).

Cortical contributions to the last-order motorneurons have been extensively investigated in the past, mostly through the analysis in the frequency domain of the coupling, between brain activity (electroencephalography, EEG or magnetoencephalography, MEG) and muscular activity (electromyography EMG, surface or intramuscular; Conway et al. 1995; Donoghue et al. 1998; Salenius and Hari 2003; Salenius et al. 1997; Schoffelen et al. 2005; Kristeva et al. 2007; Patino et al. 2008; Groß et al. 2000; Petersen et al. 2012). In this context, the measure mostly used for the assessment of cortico-spinal synchronization is *coherence*, which is an indicator ranging from 0 to 1, where 1 indicates the perfect linear correlation between two signals at a particular frequency. The linear correlation between oscillations in the motor cortex and the rhythmic discharge in the myoelectric recordings has been assessed through the use of the so-called cortico-muscular coherence (CMC). Despite the different frequency bands that have been identified in different studies, together with the various interpretations that have been drawn (Brown 2000), there is a general agreement that motor unit synchronization in the beta (15–30 Hz) and gamma (30–80 Hz) bands reflects the mediation by the cortico-spinal pathway of the communication between the brain and the muscle (Mima and Hallett 1999). It has been also shown that the coherent contribution in the beta range, visible during isometric or slowly varying contractions, shifts toward the gamma range in dynamic conditions to rapidly integrate information and in order to produce the appropriate motor commands (Omlor et al. 2007). These results have been recently confirmed in the study of cortico-muscular coherence during isotonic exercises in lower limb muscles (Gwin and Ferris 2012).

Coherence analysis has been performed also on muscle pairs (intermuscular coherence, IMC) and has been shown to reflect cortical, subcortical and spinal mechanisms (Grosse et al. 2003; Norton and Gorassini 2006) in the previously mentioned beta and gamma bands (Brown et al. 1999; Clark et al. 2013). This suggests that EMG–EMG coherence may reveal the presence of shared neural presynaptic input from higher brain structures and particularly from the motor cortex (Bo Nielsen 2002; Conway et al. 1995; Farina and Negro 2015).

Nevertheless, IMC is supposed to reflect also common contributions from the spinal interneurons that cannot be observed in the EEG-EMG coherence (Grosse et al. 2002) and can be used during dynamic cyclic tasks to give an insight into the nature of the mechanisms controlling these movements.

In the past, much attention has been paid to the study of the central pattern generators (CPGs), defined as the neural network responsible for the timing cues of a rhythmic motor output pattern (Bässler 1986). Their functioning stands out as a well-characterized, conserved vertebrate model of a neural network (Smith et al. 2013), which produces synchronized oscillations responsible, among different repetitive movements, for rhythmic locomotion and cyclic propulsion. Previous studies on animal models have prompted the theory that the CPG structures used for locomotion or any other coordinated rhythmic movement are characterized by two essential components: an oscillator for the generation of the basic rhythm and a pattern generator for the shaping of that rhythm into a spatiotemporal pattern of signals that is delivered to the muscles (Lennard and Hermanson 1985; Perret and Cabelguen 1980). In particular, the rhythm generation structure, according to Burke et al. (2001), is embodied in two reciprocally organized half-centers whose outputs are delivered to the ultimate targets (last-order interneurons that excite or inhibit spinal motorneurons) through a system of neurons that produce the required spatiotemporal sequence of commands.

In this view, and by taking into account the redundancy of the musculoskeletal system, a number of studies have hypothesized that the central nervous system (CNS) simplifies motor control by combining low-dimensional spatiotemporal structures of muscle co-activation (Bizzi et al. 2008) in order to overcome the problem of multiple degrees of freedom (Bernstein 1967). Muscle synergies are low-dimensional modules of muscle activation that—adjusted in time and amplitude—are able to accurately represent various patterns of muscle coordination during movement execution. When the coordinated activity of these groups of muscles is linked to the stabilization of physical task-related variables, they have been defined as "M-modes" (Krishnamoorthy et al. 2003; Danna-dos-Santos et al. 2007). Muscle synergies have been studied for a variety of rhythmic and discrete motor tasks under different conditions in both humans and animals (Bizzi et al. 2008; d'Avella and Lacquaniti 2013; Cappellini et al. 2006).

While muscle synergies are a representation of the overall muscular activity during a given task—regardless of the supra-spinal or spinal structures commanding this activity—when applied to rhythmic stereotypical tasks, they can give an insight into the overall structure of the CPGs (Ivanenko et al. 2005). Previous studies on walking have reported the presence of IMC only within the same muscles or between close synergists, thus concluding that during walking the muscles are activated independently due to the absence of synchronization in the time domain and in the frequency domain between muscles acting across different joints

(Bo Nielsen 2002; Hansen et al. 2001). However, recent studies on posture highlighted the existence of synchronization in the frequency domain during a postural task, with this synchronization being present among muscles acting across different and independent joints of the lower limb (Danna-Dos-Santos et al. 2013, 2015). Interestingly, the group of muscles analyzed in (Danna-Dos-Santos et al. 2013) was identified as a functional M-mode in a previous work by the same group (Danna-dos-Santos et al. 2007), so that the synchronization between different muscles could be a neural expression of functional co-activation, and it might involve also muscles that are anatomically and functionally different (Danna-Dos-Santos et al. 2015).

Given these complementary perspectives, it is of interest to study the link between synergies, synchronization and how these are influenced by the task. In this study, we aim at assessing the presence of IMC among muscles that have been previously shown to be synergistic during a free pedaling task (Hug et al. 2010; De Marchis et al. 2013a). Under the hypothesis that the presence of intermuscular synchronization during this task could be mainly related to cortical command and activity of the CPGs, IMC could provide a frequency domain correlate of temporal modular control by the CNS and has the potential to provide more direct information on the underlying neural mechanisms of rhythmic lower limb control both at the cortical and spinal level.

## Materials and methods

### Participants

Eleven subjects (27.4 ± 2.5 years) performed a pedaling exercise on an aerodynamically braked cycle-simulator. The subjects did not report any previous history of lower limb pathology or surgery and were chosen as untrained in pedaling exercise. The participants agreed to participate by signing an informed consent. The experimental procedure was carried out in accordance with the principles of the Declaration of Helsinki.

### Experimental protocol

The experimental protocol carried out for this study has been previously reported (De Marchis et al. 2013a). Summarizing, participants accomplished the motor task on an aerodynamically braked cycle-simulator equipped with instrumented pedals and standard 0.17-m cranks. After performing a 10-min warm-up and a 10-s all-out sprint to determine the maximal power output, subjects were instructed to pedal for 2 min with a self-selected strategy and a freely chosen cadence (67.3 ± 5.7 rev*min$^{-1}$, 120.6 ± 20.1 W). The protocol was modeled in order to minimize the effects of muscular fatigue (Castronovo et al. 2013).

### EMG recordings

Surface EMG signals were recorded from the following eight muscles of the dominant leg (defined as the leg the subjects usually used to kick a ball): gluteus maximus (Gmax), biceps femoris long head (BF), gastrocnemius medialis (GAM), soleus (SOL), rectus femoris (RF), vastus medialis (VM), vastus lateralis (VL) and tibialis anterior (TA). These muscles were chosen as they have been judged representative of the main muscle groups acting across the main degrees of freedom involved in cycling (Hug and Dorel 2009). EMG signals were recorded using a wireless system equipped with eight bipolar wireless electrodes (BTS FREEEMG, btsbioengineering.com), sampled at 1000 samples/s and digitized at 14 bits.

### EMG signal processing for synergy extraction

Each EMG signal was filtered in the band (20–400 Hz), full-wave-rectified and low-pass-filtered at 5 Hz in order to obtain the signal envelope. Then, each envelope was normalized with respect to the median peak across all the consecutive pedaling cycles, in order to exclude the contribution of occasional peaks of activation. For each subject, muscle synergies were extracted by applying nonnegative matrix factorization (*NMF*, Lee and Seung 1999) to the $M_{8\times N}$ matrix containing the EMG envelopes of the whole trial for the eight muscles and for the $N$ samples (60 pedaling cycles on average for each subject). Briefly, *NMF* factorizes $M$ into an approximated form $M \approx WxH$, where $W$ is a $8 \times k$ matrix of the synergy vectors, containing the spatial information of muscle co-activation, $H$ is a $k \times N$ matrix of the synergy activation coefficients, containing the temporal information of synergy recruitment, and $k$ is the number of extracted muscle synergies. *NMF* iteratively minimizes the matrix norm $||M-WH||$ through the use of simple multiplicative update rules. The number of synergies $k$ is chosen before the application of *NMF* according to the amount of explained variance for each $i$-th muscle EMG envelope, defined as:

$$VAF_i = 1 - \frac{\sum_{j=1}^{N} \left(M_{ij} - R_{ij}\right)^2}{\sum_{j=1}^{k} \left(M_{ij}\right)^2} \quad (1)$$

where $i$ denotes the $i$-th muscle, and $R = WxH$ is the matrix resulting from the reconstruction with $k$ synergies. The number of extracted synergies was varied between one and eight for $VAF_i$ calculation, and $k$ was chosen as the smallest number able to explain at least the 90 % of $VAF_i$ for each muscle. Additional synergies were not extracted if the

muscle with the lowest $VAF_i$ showed an increase in VAF lower than 5 % when extracting $k + 1$ synergies (Clark et al. 2010). This strict approach ensures a detailed reconstruction of the original EMG envelopes for each subject.

### EMG preprocessing for coherence analysis

The preprocessing for coherence calculation did not include any band-pass filtering of the EMG signal: this was done in order to avoid any effect of filtering on the coherence estimation and in order to preserve the low-frequency bands that could be involved in coherent contributions (Kattla and Lowery 2010; Poston et al. 2010). EMG signals were visually inspected to check the absence of any artifact and detrended. Due to the dynamic nature of the studied task, the EMG slow amplitude modulation at the pedaling frequency constitutes an artifact in the estimated EMG–EMG coherence spectrum, and it also constitutes a limit for coherence calculation, due to the stationarity requirements. For the previous reasons, the low-frequency EMG amplitude modulation was removed by using an amplitude demodulation approach as proposed by (Boonstra et al. 2009). The mean value of each raw EMG signal was removed, and the analytic signal was calculated as follows:

$$\mu(t) = x(t) + ix_H(t) = A(t)e^{i\theta(t)} \tag{2}$$

where $x_H(t)$ is the Hilbert transform of $x(t)$, $A(t)$ is the time-dependent amplitude modulation of the underlying process, and $\theta(t)$ is the instantaneous frequency of the analytic signal defined as:

$$\theta(t) = \tan^{-1}\left[\frac{x_H(t)}{x(t)}\right] \tag{3}$$

As shown in (Boonstra et al. 2009), the demodulated version of the original signal $x(t)$ can be obtained as:

$$x_D(t) = \cos\left[\theta(t)\right] \tag{4}$$

The values of $x_D(t)$ span the range $[-1 \div 1]$ and constitute an estimation of the underlying point process without the contribution of the slow amplitude modulation component $A(t)$.

### Selection of synergy activation periods and muscle pairs

Within each extracted synergy, a group of muscles for subsequent coherence analysis was selected on the basis of their relative contribution to that synergy. In particular, each muscle synergy vector $W$ was normalized with respect to the value of the most active muscle within that synergy, in order to assume values in the range [0–1]. After normalization, a muscle was considered as active within a synergy if its contribution to the synergy vector $W$ was higher than 0.25. Based on recent results (De Marchis et al. 2013a), due to the stability of the muscle synergy vectors across subjects, only the average synergy vectors were taken into account, as they have been shown to be representative of the muscle coordination for all the subjects. Synergy activation coefficients $H$ were then extracted by using nonnegative reconstruction (Muceli et al. 2010; De Marchis et al. 2013b) by fixing the average muscle synergies and let only $H$ update at every iteration of the NMF algorithm.

In order to perform coherence analysis only within the periods of synergy activation, a threshold on the synergy activation coefficients $H$ was placed: a group of muscles as individuated in each $W$ was considered co-active only when the synergy activation coefficient was higher than its mean value. EMG signals within the previous time periods were selected for subsequent coherence analysis (Fig. 1): in particular, for each EMG signal and for each synergy, a time series $x_{DC}(t)$ was constructed by concatenating the parts of EMG signal within the synergy activation period. In order to avoid abrupt changes of the $x_{DC}(t)$ time series within the concatenation points, each independent EMG segment was multiplied by a Hanning window of the same length before demodulation.

### EMG–EMG coherence among synergistic muscles

Within each muscle synergy, $x_{DC}(t)$ for each muscle within the selected activation periods was used to calculate the coherence function between each pair of active muscles belonging to the same muscle synergy. Coherence between two EMG signals was calculated as follows:

$$C_{xy}(f) = \frac{\left|P_{xy}(f)\right|^2}{|P_{xx}(f)|\left|P_{yy}(f)\right|} \tag{5}$$

where $P_{xy}(f)$ is the power cross-spectral density, and $P_{xx}(f)$ and $P_{yy}(f)$ are the power spectral densities of the two EMG signals. In order to provide a unique function describing the neural coupling between muscles belonging to the same synergy, we used the pooled coherence function that was first proposed by (Amjad et al. 1997) and defined as follows:

$$C_{\text{pool}}(f) = \frac{\left|\sum_{j=1}^{p} P_{xy_j}(f)L_j\right|^2}{\left(\sum_{j=1}^{p} P_{xx_j}L_j\right)\left(\sum_{j=1}^{p} P_{yy_j}L_j\right)} \tag{6}$$

where $p$ is the number of muscle pairs from which coherence has been estimated, $j$ denotes the $j$-th pair of muscles, and $L_j$ is the number of segments used for coherence estimation for the $j$-th muscle pair. In case of a single synergy vector $W$, since the number of segments $L_j$ is common to every coherence estimation, $C_{\text{pool}}$ is the average $C_{xy}$ among the $p$ muscle pairs emerging from that synergy. Coherence

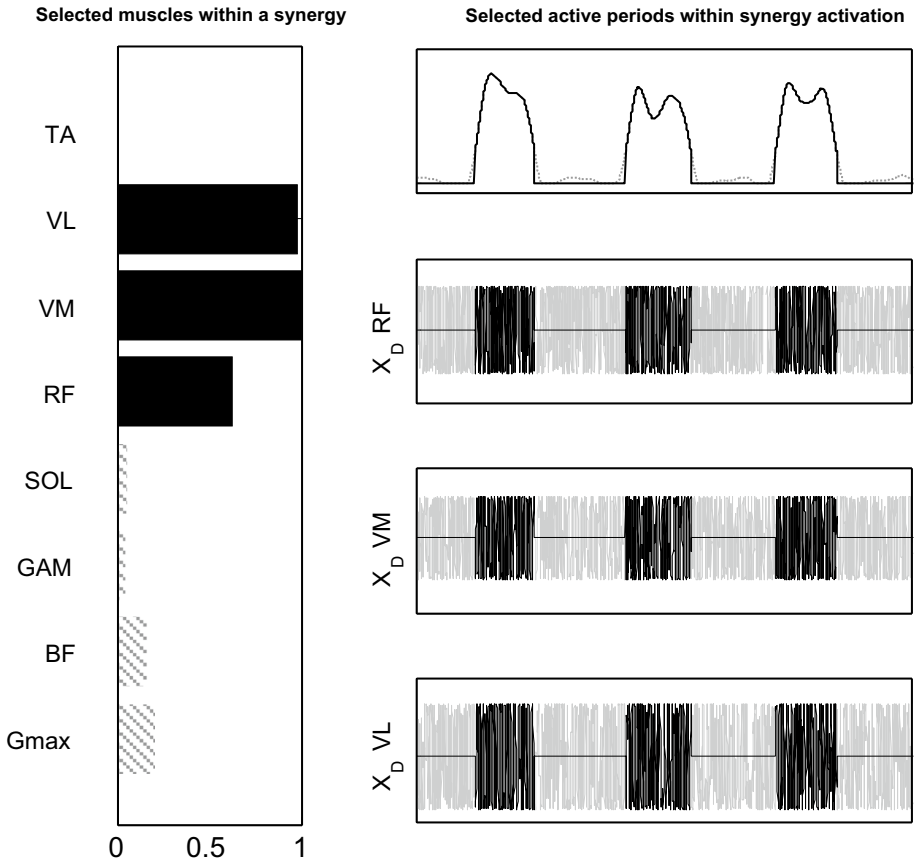


**Fig. 1** Example of muscle selection and time interval selection within a muscle synergy. Only RF, VM and VL are selected from the synergy vector in the *left bar plot*. After this, their demodulated EMG is taken only within the synergy activation periods, as indicated in the *upper plot*

estimation, both for analysis between two muscles and for pooled analysis, was based on the use of overlapping segments (Welch 1967), for two main reasons: (1) selection of the synergy activation periods significantly reduces the length of the analyzed time series, and (2) the use of overlapping segments has been shown to improve coherence estimation (Terry and Griffin 2008). Each coherence spectrum was thus estimated with 500-ms Hanning windows with 50 % overlapping, leading to a spectral resolution of 2 Hz and doubling up the number of available segments. This combination of window width and overlapping was used for the calculation of both the coherence spectra in Eq. (5) and the pooled coherence in Eq. (6). For pooled coherence analysis, we assume that the phase difference between different pairs of synergistic muscles is identical.

## EMG–EMG coherence among partially co-active, non-synergistic muscles

In order to verify the conceptual validity of the pooled coherence obtained within muscle synergies, we applied a cross-synergy analysis of coherence involving pairs of co-active but non-synergistic muscles (i.e., pairs of muscles belonging to different muscle synergies having a partially co-active synergy activation coefficient $H$). Once the periods of activation of each synergy were identified according to the procedure described in "Selection of synergy activation periods and muscle pairs" section, a co-activation rate parameter $CR$ between two generic synergies $A$ and $B$ was calculated as follows:

$$CR_{AB} = \frac{ACT_A \cap ACT_B}{ACT_A \cup ACT_B} \tag{7}$$

where $ACT$ denotes the periods of activation of a synergy. A pair of non-synergistic muscles was considered co-active if the corresponding synergy activation periods had $CR > 0.15$. Each pair of co-active muscles underwent coherence analysis.

### *Time-domain synchronization*

Within each synergy activation period, the cross-correlogram was calculated between each pair of $X_{DC}(t)$ belonging to that synergy. The absolute value of the unbiased cross-correlogram was used as a measure of time-domain synchronization.

Also a pooled measure of time synchronization $R_{\text{pool}}$ was calculated, in a similar way as it was described for coherence estimates in "EMG–EMG coherence among synergistic muscles" section.

### Statistical analysis and significance of the estimated synchronization measures

Each estimated $C_{xy}$ and $R_{xy}$ value underwent Fischer transformation in order to normalize the coherence contributions and cross-correlogram values and to allow the comparison among different participants as follows:

$$Z_{xy}(f) = \sqrt{2L}\tanh^{-1}\left(\sqrt{C_{xy}(f)}\right) \quad (8)$$

Significance of the estimated coherence spectra and time-domain correlation was assessed by using a surrogate data analysis: in particular, for each pair of preprocessed EMG signals (see "EMG Preprocessing for coherence analysis" section), surrogate series were generated by calculating the Fourier transform, independently shuffling the phase components, and calculating the inverse Fourier transform (Faes et al. 2004; Severini et al. 2012). This procedure for generating surrogate data ensures the preservation of the power spectrum of each signal, but makes the two series completely uncorrelated in the time and frequency domain. For each $C_{xy}$ and $R_{xy}$ estimation, 50 surrogate EMG signals were used to calculate a set of coherence spectra and correlograms expected from chance. The significance threshold was set at 95 % percentile.

$C_{\text{pool}}$ for each extracted muscle synergy was analyzed within four different frequency bands. An average Z-coherence value $I_{CZ}$ was calculated for each $C_{\text{pool}}$ spectrum as follows:

$$I_{CZ}(f_1,f_2) = \frac{1}{(f_1 - f_2)}\int_{f_1}^{f_2} C_{\text{pool}}(f)\mathrm{d}f \quad (9)$$

where $f_1$ and $f_2$ are the lower and upper bound of each of the following frequency bands: (0–5, 5–15, 15–30 and 30–60 Hz). The aforementioned frequency bands—generally related in literature to the EEG activity—have frequently been used for the evaluation of EEG/MEG-EMG (Conway et al. 1995; Brown et al. 1998; Halliday et al. 1998) and EMG–EMG coherence (Grosse et al. 2002; Semmler et al. 2013).

## Results

Four synergies were extracted for all the subjects according to the 90 % $VAF_i$ criterion. Synergy $W_1$ consists of the joint activation of the quadriceps muscles (VM, VL and RF), synergy $W_2$ consists of the co-activation of angle plantar flexors (GAM and SOL) together with Gmax, synergy $W_3$ co-activates two bi-articular knee flexor muscles (BF and GAM), while synergy $W_4$ is composed by the activity of RF and TA. The spatiotemporal structure of the extracted muscle synergies is reported in the top panels of Fig. 2, with the detailed duration of synergy recruitment within the pedaling cycles indicated in Table 1. Muscles in synergies $W_1$ and $W_2$ underwent pooled coherence and cross-correlation analysis, since they are composed of three significantly active muscles, while muscles in synergies $W_3$ and $W_4$ underwent a simple muscle pair coherence analysis, since only two muscles form the synergy.

### Frequency domain coupling

Pooled coherence estimates highlight a significant coherence peak in the gamma band (30–60 Hz) only for synergy $W_1$. This pooled coherence derives from a regular coherence profile for all the single muscle pairs forming the synergy (RF/VM, RF/VL and VM/VL.). The other synergies do not show significant coherent contributions within any of the analyzed frequency bands (Fig. 2), apart from synergy $W_2$, which shows a significant peak around 3–4 Hz, mainly due to the GAM/SOL muscle pair and, to a lesser extent, to the Gmax/GAM pair.

When taking into account the integral Z-coherences as a measure of coherence power in different bands (Fig. 3), only synergy $W_1$ also presents a significant contribution in gamma band. This gamma band coherent contribution has been identified within the periods of activation of synergy $W_1$ (RF–VM–VL), where most of the force is applied to the pedal (De Marchis et al. 2013a, b).

Concerning the cross-synergy coherence analysis, a co-activation rate higher than 15 % is present between the pair of synergies ($W_1$–$W_2$), ($W_1$–$W_4$) and ($W_2$–$W_3$), indicating that these pairs of synergies are partially co-recruited during the pedaling cycle. The other pairs of synergies present a minimal but negligible co-activation, as indicated in Table 2. Coherences calculated between the corresponding pairs of muscles highlight that there is no significant coupling within the bands taken into account for pairs of co-active but non-synergistic muscles (Fig. 4).

### Time-domain synchronization

Time-domain analysis, as individuated by pooled cross-correlograms, reveals the presence of synchronization for synergies $W_1$ and $W_2$. However, while this time-domain synchronization is consistent across all the muscle pairs for $W_1$ (RF–VM–VL), the significant pooled cross-correlation of $W_2$ mainly derives from the high synchronization between GAM and SOL. No synchronization is present for the other muscle pairs belonging to synergies $W_3$ and $W_4$ (Fig. 5).

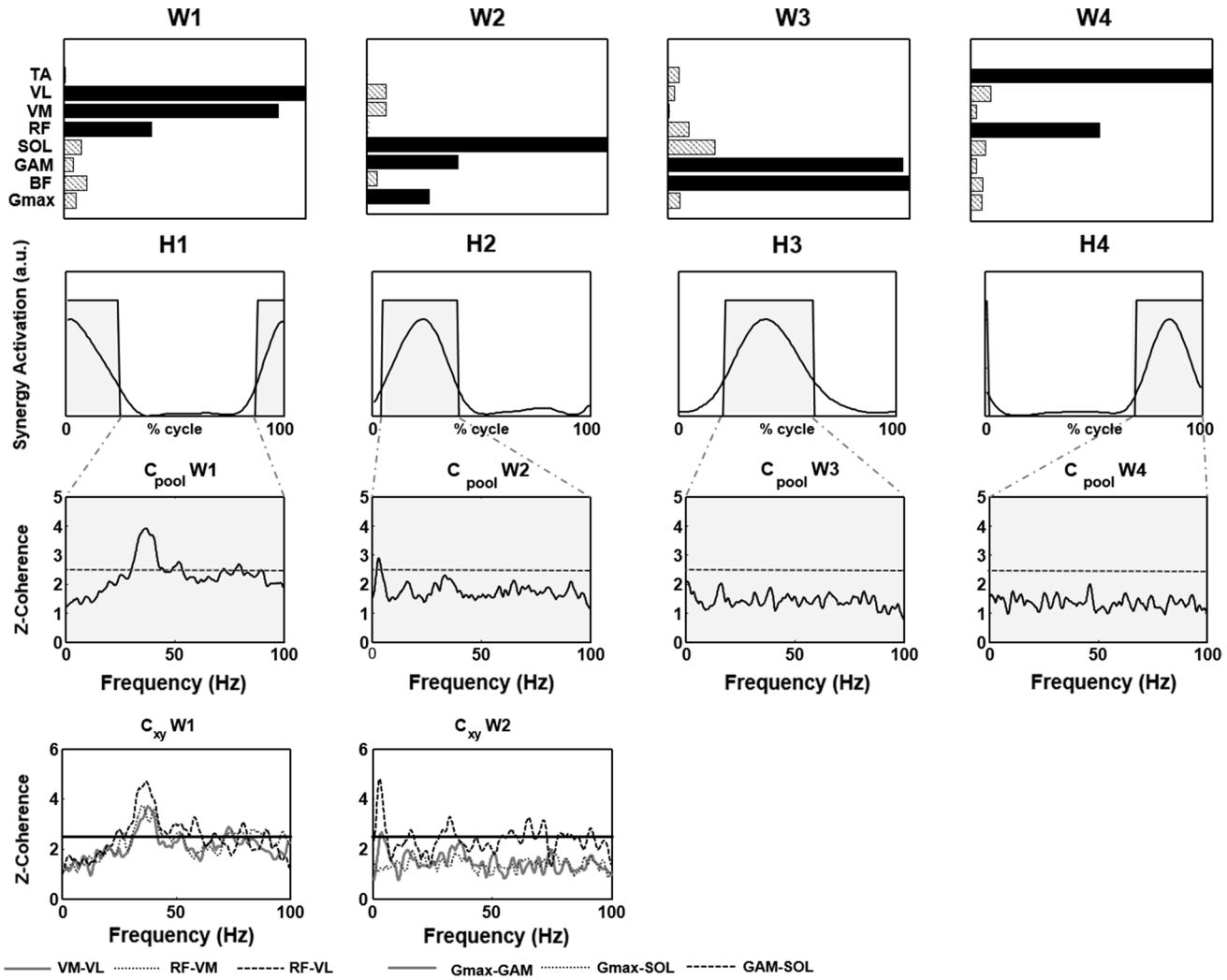


**Fig. 2** *Upper row*: muscle synergy vectors averaged across the eleven participants. These vectors have been used to select the muscles used for the computation of the pooled coherence. *Second row*: average synergy activation coefficients, plotted against integer percentages of the pedaling cycle. These time-varying activation coefficients have been used to select the time periods in which coherence has been calculated (indicated with a *gray area* in the figure). *Third row*: pooled coherence profiles averaged across the eleven subjects for each muscle synergy within the selected activation periods. *Horizontal thick line* indicates the significance level. *Fourth row*: average single muscle pair coherence estimates for the synergies composed by more than two muscles

**Table 1** Duration of the synergy activation coefficients within the pedaling cycles for the four identified muscle synergies (mean ± std across subjects)

| Synergy activation | Duration (mean ± std) ms |
|---|---|
| H1 | 412 ± 37 |
| H2 | 377 ± 64 |
| H3 | 331 ± 74 |
| H4 | 275 ± 34 |

## Discussion

The main finding of this work is the presence of intermuscular coherence in the gamma band for anatomically close synergistic muscles acting on the extension of the knee during the pedaling task. In addition to that, a significant peak around 3–4 Hz was also noticed for close bi-articular muscles acting on the knee and ankle. The use of coherence analysis within motor modules extracted through NMF algorithm thus highlights the existence of correlated neural

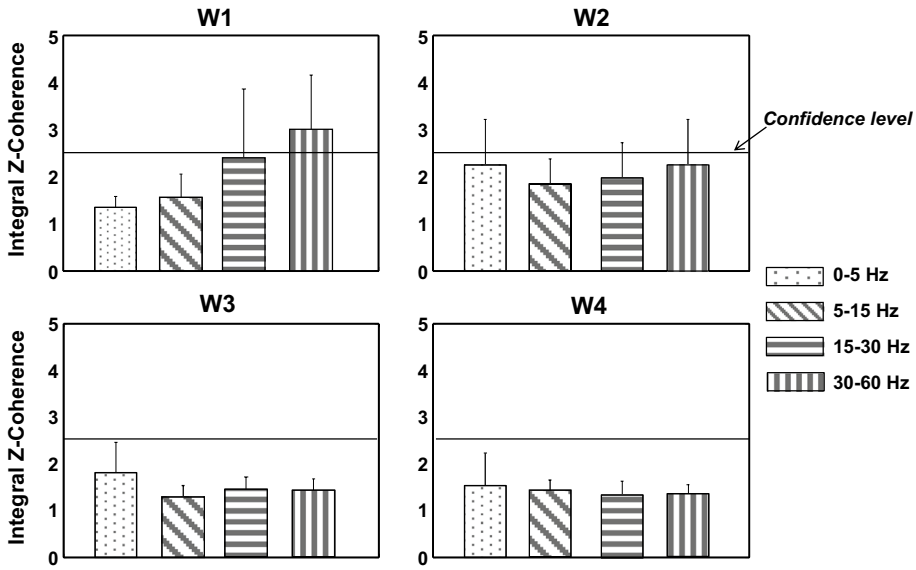


**Fig. 3** Averaged integral Z-coherences calculated within four different frequency bands: 0–5, 5–15, 15–30 and 30–60 Hz. *Horizontal lines* indicate the threshold level for pooled coherence significance for each muscle synergy. The only significant contribution is present for the first muscle synergy (RF, VM and VL) in the gamma band

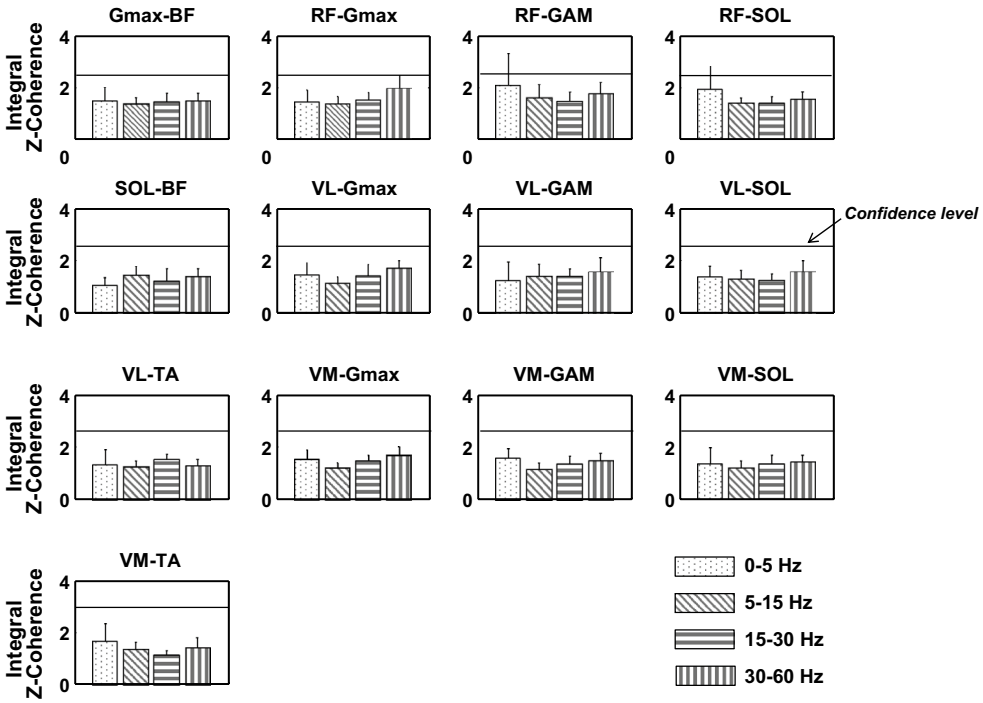


**Fig. 4** Cross-synergy analysis. Average integral Z-coherences calculated between pairs of co-active but non-synergistic muscle pairs within the four analyzed frequency bands. *Horizontal line* indicates the threshold for statistical significance. No significant coherence is present for all the muscle pairs within all the analyzed frequency bands

inputs only for a specific group of synergistic muscles during the analyzed dynamic motor task. These findings will be discussed from a neurophysiological, neuromechanical and anatomical point of view, but also the technical aspects regarding IMC calculation will be discussed in detail, since they can significantly affect the results and their neurophysiological interpretation.

## Neurophysiological, neuromechanical and anatomical correlates of the observed intermuscular coupling

Hansen et al. (2001) identified a correlation in the frequency domain in the lower limbs during walking. In particular, they found significant contributions for all muscles at the frequency of the task (<5 Hz), due to the repetition

**Table 2** Co-activation rates between the identified synergies

| | H1 | H2 | H3 | H4 |
|---|---|---|---|---|
| H1 | | *0.47* | 0.05 | *0.19* |
| H2 | | | *0.21* | 0.03 |
| H3 | | | | 0.03 |

Pairs of non-synergistic muscles were considered as co-active if the co-activation rate between of the corresponding synergies was higher than 0.15 (indicated in italic). Three pairs of synergies share some temporal activation intervals (W1/W2, W1/W4 and W2/W3)

rate and in the lower beta band only between anatomically close muscles, but not for distant ones, even if co-activated. This latter contribution has been interpreted as communality between the driving inputs to motorneurons coming from common last-order interneurons in the spinal tract (Bo Nielsen 2002). At the same time, for most of the muscles it appears that motorneurons are activated relatively independently and do not share a common input from higher levels. Norton and Gorassini (2006) investigated higher-frequency contributions to IMC in subjects affected by incomplete spinal cord injuries during walking. They were able to find such contributions during the stance phase for co-activating muscles. Moreover, the power in the 24–40 Hz band in these subjects was proportional to the amount of muscle strength. Thus, this contribution has been further related to the activation of supra-spinal circuits. This is not unexpected given the additional control needs of incomplete spinal cord injury patients in the walking task.

In this study, we report significant contributions, only for topologically close synergistic muscles, while no linear phase dependency is observed for distant muscles, even if co-activated. A possible interpretation to such observation could be that spinal circuits do not share common last-order input to their motorneurons. In this case, the present results would suggest some insights on the actual structure of central pattern generators. Recent studies on the topology of central pattern generators in animal models have proposed a multi-level structure. In particular, Zhong et al. (2012) have recently proposed a two-level structure where the higher level, constituted by Type I V2a interneurons, represents the rhythm generators that "synergistically" activate pattern formation structures (Type II V2a interneurons) that, on the other end, activate synergistic muscles together.

Pairing this observation with the theory of muscle synergies, especially during rhythmic movements of the lower limbs such as walking and cycling (and excluding cortical command and reflex activity), the activation patterns of the synergies can be seen as the rhythmic activation of the rhythm generators, while the weight of the synergy can be seen as a last-level "photograph" of the pattern formation structures. Then, assuming that the task is completely CPG-based, the presented results would suggest that muscles of

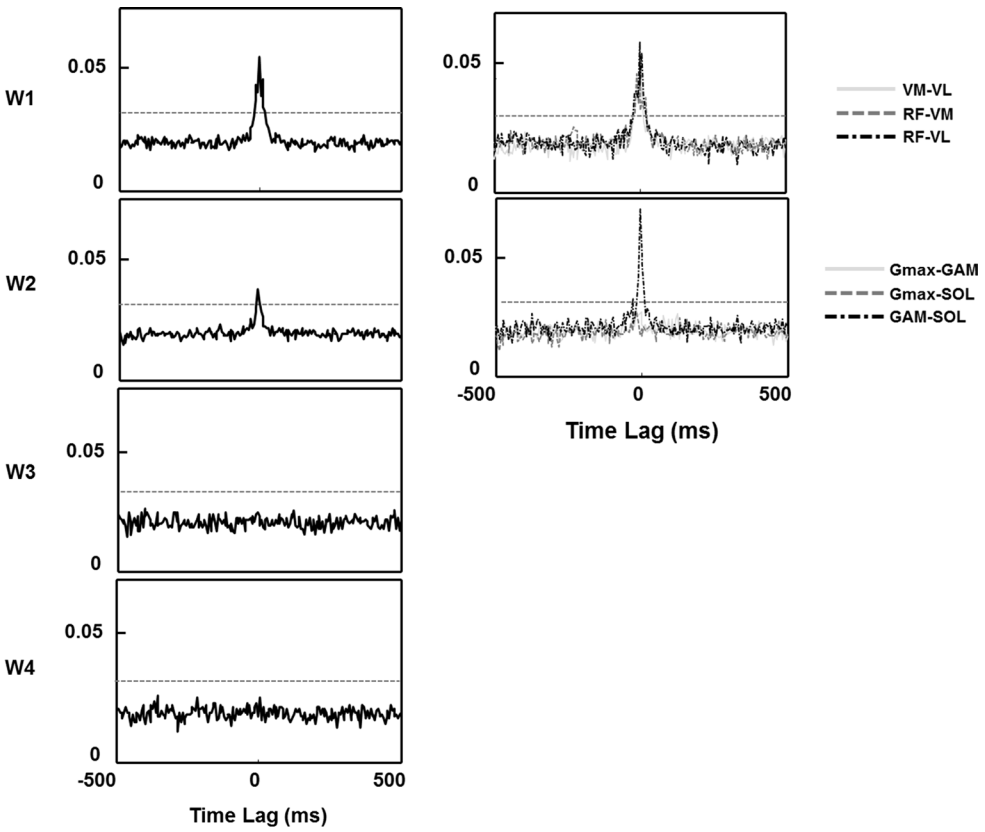


**Fig. 5** Time-domain synchronization, identified through cross-correlation analysis averaged across participants. Significant time synchronization is visible for synergies #1 and #2 (confidence level shown as *dotted line*)

$W_1$ share common input from the same pattern formation structures, while those of $W_2$, $W_3$ and $W_4$ do not share the same lower-level input, with the exclusion of the GAM/SOL muscle pair.

Another interpretation may be that spinal rhythms are not expressed in IMC and what we observed is the cortical activity related to $W_1$, which is the synergy mainly related to force production. The presence of gamma intermuscular coherence could be explained by the need of rapidly integrating information and producing the appropriate motor commands in a dynamic scenario, and it might thus reflect a cortico-muscular coupling within the same bands between cortical activity and the single muscles.

In this light, these coherent contributions might have a functional significance when related to the biomechanics of pedaling: the muscle groups which act as force producers during the pedaling action show coherence contributions within higher-frequency bands. The presence of a coherent contribution within the gamma (30–60 Hz) band is in line with previous studies analyzing tasks in which a dynamic force output was present (Omlor et al. 2007). On top of that, from a neuromechanical point of view, it is also possible that in the cycling task there is a stabilization of some performance variable that is carried out by the first synergy and that may be why a significant coherent contribution emerges.

Similarly, the low-frequency coherence contributions observed in the muscles of $W_2$ and especially in the couple GAM/SOL could be functionally related to the stabilizing function that these muscles have on the ankle joint during the propulsion phase. On the other hand, the presence of such contributions around 3–4 Hz does not match with results previously found in literature.

The absence of coherent contributions for all the other identified modules could be attributed to different factors. This lack of communality in the frequency domain could be due to the fact that these other groups of muscles are co-activated in a regular way but without any stabilization function or without any significant task-related aim. In fact, the other leg works as power producer when the functional action of the first is concluded. Thus, it might be possible that the muscles belonging to $W_1$ form a functional muscle synergy during pedaling, with the aim of stabilizing a performance variable in the task space (Scholz and Schöner 1999; Danna-Dos-Santos et al. 2007). This aspect related to neural synchronization in the frequency domain together with the statistical regularity of muscle co-activation in the time domain needs further studies, in order to explore more in detail the possible neural organization of functional muscle synergies.

From an anatomical point of view, it is necessary to notice that the muscles of $W_1$ (VM, VL, RF), that are the muscles forming the quadriceps, are not completely independent. These muscles in fact share a function of knee extension in a big variety of tasks (walking, jumping, sit-to-stand, squat). These muscles also share the same innervation from the femoral nerve, with projections to the L2–L4 spinal levels. This communality may be the reason behind the significant coherence contributions we found for these muscles. A similar remark can be done for the muscles of the triceps surae (GAM, SOL) that are encoded in $W_2$. These muscles are functionally tied in several tasks and share the same innervation (sural nerve) and spinal projection (S1–S2; Ivanenko et al. 2005). Similarly, also $W_1$ and $W_2$ are constituted by both mono-articular (VM/VL for the quadriceps, GAM for the surae) and bi-articular (RF for the quadriceps, SOL for the surae) muscles. From a biomechanical point of view, the two aforementioned bi-articular muscles play a multiple role during pedaling: while RF contributes both to knee extension (W1) and combined hip/ankle extension ($W_4$ in synergy with TA), GAM plays its major role during knee flexion ($W_3$) rather than ankle plantar flexion ($W_2$).

Moreover, by looking at $W_2$, significant synchronization is observed mainly for the GAM/SOL muscle pair, with negligible contributions of the Gmax. In this light, topological factors may be one of the reasons behind the presence of coherence only for subsets of muscles during the pedaling task, while the frequency content of these coherence contributions is possibly related to the different functional task (force production for $W_1$, stabilization for $W_2$). Nevertheless, previous studies have found significant coherence in synergistic topologically distant muscles that do not share the same innervation during balance (Danna-Dos-Santos et al. 2013, 2015).

Based on these observations, both anatomical and functional aspects might contribute to the formation of synchronized intermuscular patterns.

### Technical aspects regarding IMC calculation

With respect to most of the previous studies analyzing intermuscular coherence through the EMG signal, which usually applied a rectification to the EMG signal before calculating coherence, this is one of the few studies that calculate coherence on the demodulated raw EMG signal (Boonstra et al. 2009). This signal should reflect the underlying point process without the contribution of the modulation due to time-varying force production typical of dynamic motor tasks. EMG rectification has often been seen as a necessary step for the calculation of cortico-muscular and intermuscular coherence, but recent studies have demonstrated that this assumption might be incorrect under specific circumstances, as there has been much debate lately in literature regarding the suitability of rectification while investigating intermuscular and cortico-muscular

coherence (McClelland et al. 2012; Farina et al. 2013; Boonstra and Breakspear 2012). Farina et al. (2013) effectively demonstrated that EMG amplitude cancellation affects the estimation of coherence and that rectification is indicated only in tasks consisting of low-level contractions. This is further confirmed by the results obtained by Boonstra and Breakspear (2012), where it is theoretically demonstrated that EMG rectification affects the calculation of coherence when the MUAP shapes are uniform, and this is likely because MUAP shapes uniformity increases EMG cancellation (Farina et al. 2008).

In view of these considerations, we decided not to include the rectification of the EMG signal in our analysis. In particular, we limited the treatment of the signal to the demodulation directly applied to the raw EMG signal, without the rectification used in Boonstra et al. (2009). Demodulation has been applied to cancel the slow fluctuation of the overall EMG amplitude due to the cyclical nature of the studied task. Given this transformation, together with the overall cyclostationarity of the EMG signal (Bonato et al. 2001), we assume that stationarity requirements for coherence analysis are met.

Another reason for not using the signal rectification is related to the aim of the analysis. IMC, in fact, involves signals of the same nature and with the same frequency content, and rectification was thus excluded in order not to introduce further steps whose effects are still unclear. We are anyway conscious that the different treatment of the signal may affect the frequency components of the extracted IMC, limiting the comparability with the other studies on CMC and IMC that use rectification or do not use demodulation technique.

## Conclusions

In this study, we analyzed the neural synchronization between EMG signals recorded from synergistic muscles. The outcome of traditional nonnegative matrix factorization algorithm highlights a modular organization of a free-cycling task based on four muscle synergies. By taking into account the intermuscular synchronization within the periods of co-activation, it has been shown that a significant intermuscular coherence is only present for one out of the four identified muscle synergies. This identified coherent contribution is present in the gamma band, and it is in line with previous studies targeting dynamic motor tasks, suggesting the possible cortical origin of this intermuscular coupling. The only muscle synergy showing significant coherence is composed by the group of muscles forming the quadriceps, mainly responsible for force production and crank propelling during the pedaling cycle. This finding suggests that intermuscular coupling generally observed during different movement in humans might reflect the functional role of a co-active group of muscles, as for example the stabilization of a task-relevant variable, besides the anatomical constraints deriving from common spinal projections. However, although our results seem to support more the cortical than the spinal involvement, further investigation is required to deeply understand the CPG contribution to the studied task.

**Conflict of interest** We declare that we have no conflict of interest with the present manuscript.

## References


Amjad AM, Halliday DM, Rosenberg JR, Conway BA (1997) An extended difference of coherence test for comparing and combining several independent coherence estimates: theory and application to the study of motor units and physiological tremor. J Neurosci Methods 73(1):69–79

Bässler U (1986) On the definition of central pattern generator and its sensory control. Biol Cybern 54(1):65–69

Bernstein NA (1967) The co-ordination and regulation of movements. Pergamon, Oxford

Bizzi E, Cheung VCK, d'Avella A, Saltiel P, Tresch M (2008) Combining modules for movement. Brain Res Rev 57(1):125–133

Bo Nielsen J (2002) Motoneuronal drive during human walking. Brain Res Rev 40(1):192–201

Bonato P, Roy SH, Knaflitz M, De Luca CJ (2001) Time-frequency parameters of the surface myoelectric signal for assessing muscle fatigue during cyclic dynamic contractions. IEEE Trans Biomed Eng 48(7):745–753

Boonstra TW, Breakspear M (2012) Neural mechanisms of intermuscular coherence: implications for the rectification of surface electromyography. J Neurophysiol 107(3):796–807

Boonstra TW, Daffertshofer A, Roerdink M, Flipse I, Groenewoud K, Beek PJ (2009) Bilateral motor unit synchronization of leg muscles during a simple dynamic balance task. Eur J Neurosci 29(3):613–622

Brown P (2000) Cortical drives to human muscle: the Piper and related rhythms. Prog Neurobiol 60(1):97–108

Brown P, Salenius S, Rothwell JC, Hari R (1998) Cortical correlate of the Piper rhythm in humans. J Neurophysiol 80(6):2911–2917

Brown P, Farmer SF, Halliday DM, Marsden J, Rosenberg JR (1999) Coherent cortical and muscle discharge in cortical myoclonus. Brain 122(3):461–472

Burke RE, Degtyarenko AM, Simon ES (2001) Patterns of locomotor drive to motoneurons and last-order interneurons: clues to the structure of the CPG. J Neurophysiol 86(1):447–462

Cappellini G, Ivanenko YP, Poppele RE, Lacquaniti F (2006) Motor patterns in human walking and running. J Neurophysiol 95(6):3426–3437

Castronovo AM, Conforto S, Schmid M, Bibbo D, D'Alessio T (2013) How to assess performance in cycling: the multivariate nature of influencing factors and related indicators. Front Physiol 4:116

Clark DJ, Ting LH, Zajac FE, Neptune RR, Kautz SA (2010) Merging of healthy motor modules predicts reduced locomotor performance and muscle coordination complexity post-stroke. J Neurophysiol 103(2):844

Clark DJ, Kautz SA, Bauer AR, Chen YT, Christou EA (2013) Synchronous EMG activity in the piper frequency band reveals the corticospinal demand of walking tasks. Ann Biomed Eng 41(8):1778–1786

Conway BA, Halliday DM, Farmer SF, Shahani U, Maas P, Weir AI, Rosenberg JR (1995) Synchronization between motor cortex and spinal motoneuronal pool during the performance of a maintained motor task in man. J Physiol 489(Pt 3):917–924

Danna-dos-Santos A, Slomka K, Zatsiorsky VM, Latash ML (2007) Muscle modes and synergies during voluntary body sway. Exp Brain Res 179(4):533–550

Danna-Dos-Santos A, Boonstra TW, Degani AM, Cardoso VS, Magalhaes AT, Mochizuki L, Leonard CT (2013) Multi-muscle control during bipedal stance: an EMG–EMG analysis approach. Exp Brain Res 232(1):75–87

Danna-Dos-Santos A, Degani AM, Boonstra TW, Mochizuki L, Harney AM, Schmeckpeper MM et al (2015) The influence of visual information on multi-muscle control during quiet stance: a spectral analysis approach. Exp Brain Res 233(2):657–669

d'Avella A, Lacquaniti F (2013) Control of reaching movements by muscle synergy combinations. Front Comput Neurosci 7:42

De Marchis C, Schmid M, Bibbo D, Bernabucci I, Conforto S (2013a) Inter-individual variability of forces and modular muscle coordination in cycling: a study on untrained subjects. Hum Mov Sci 32(6):1480–1494

De Marchis C, Schmid M, Bibbo D, Castronovo AM, D'Alessio T, Conforto S (2013b) Feedback of mechanical effectiveness induces adaptations in motor modules during cycling. Front Comput Neurosci 7:35

Donoghue JP, Sanes JN, Hatsopoulos NG, Gaál G (1998) Neural discharge and local field potential oscillations in primate motor cortex during voluntary movements. J Neurophysiol 79:159–173

Faes L, Pinna GD, Porta A, Maestri R, Nollo G (2004) Surrogate data analysis for assessing the significance of the coherence function. IEEE Trans Biomed Eng 51(7):1156–1166

Farina D, Negro F (2015) Common synaptic input to motor neurons, motor unit synchronization, and force control. Exerc Sport Sci Rev 43(1):23–33

Farina D, Cescon C, Negro F, Enoka RM (2008) Amplitude cancellation of motor-unit action potentials in the surface electromyogram can be estimated with spike-triggered averaging. J Neurophysiol 100(1):431–440

Farina D, Negro F, Jiang N (2013) Identification of common synaptic inputs to motor neurons from the rectified electromyogram. J Physiol 591(10):2403–2418

Groß J, Tass PA, Salenius S, Hari R, Freund HJ, Schnitzler A (2000) Cortico-muscular synchronization during isometric muscle contraction in humans as revealed by magnetoencephalography. J Physiol 527(3):623–631

Grosse P, Cassidy MJ, Brown P (2002) EEG–EMG, MEG–EMG and EMG–EMG frequency analysis: physiological principles and clinical applications. Clin Neurophysiol 113(10):1523–1531

Grosse P, Guerrini R, Parmeggiani L, Bonanni P, Pogosyan A, Brown P (2003) Abnormal corticomuscular and intermuscular coupling in high-frequency rhythmic myoclonus. Brain 126(2):326–342

Gwin JT, Ferris DP (2012) Beta-and gamma-range human lower limb corticomuscular coherence. Front Hum Neurosci 6:258

Halliday DM, Conway BA, Farmer SF, Rosenberg JR (1998) Using electroencephalography to study functional coupling between cortical activity and electromyograms during voluntary contractions in humans. Neurosci Lett 241(1):5–8

Hansen NL, Hansen S, Christensen LO, Petersen NT, Nielsen JB (2001) Synchronization of lower limb motor unit activity during walking in human subjects. J Neurophysiol 86(3):1266–1276

Hug F, Dorel S (2009) Electromyographic analysis of pedaling: a review. J Electromyogr Kinesiol 19:182–198

Hug F, Turpin NA, Guével A, Dorel S (2010) Is interindividual variability of EMG patterns in trained cyclists related to different muscle synergies? J Appl Physiol 108(6):1727–1736

Ivanenko YP, Cappellini G, Dominici N, Poppele RE, Lacquaniti F (2005) Coordination of locomotion with voluntary movements in humans. J Neurosci 25(31):7238–7253

Kattla S, Lowery MM (2010) Fatigue related changes in electromyographic coherence between synergistic hand muscles. Exp Brain Res 202(1):89–99

Krishnamoorthy V, Goodman S, Zatsiorsky V, Latash ML (2003) Muscle synergies during shifts of the center of pressure by standing persons: identification of muscle modes. Biol Cybern 89(2):152–161

Kristeva R, Patino L, Omlor W (2007) Beta-range cortical motor spectral power and corticomuscular coherence as a mechanism for effective corticospinal interaction during steady-state motor output. Neuroimage 36(3):785–792

Lee DD, Seung HS (1999) Learning the parts of objects by non-negative matrix factorization. Nature 401(6755):788–791

Lennard PR, Hermanson JW (1985) Central reflex modulation during locomotion. Trends Neurosci 8:483–486

McClelland VM, Cvetkovic Z, Mills KR (2012) Rectification of the EMG is an unnecessary and inappropriate step in the calculation of corticomuscular coherence. J Neurosci Methods 205(1):190–201

Mima T, Hallett M (1999) Corticomuscular coherence: a review. J Clin Neurophysiol 16(6):501

Muceli S, Boye AT, d'Avella A, Farina D (2010) Identifying representative synergy matrices for describing muscular activation patterns during multidirectional reaching in the horizontal plane. J Neurophysiol 103(3):1532–1542

Norton JA, Gorassini MA (2006) Changes in cortically related intermuscular coherence accompanying improvements in locomotor skills in incomplete spinal cord injury. J Neurophysiol 95(4):2580–2589

Omlor W, Patino L, Hepp-Reymond MC, Kristeva R (2007) Gamma-range corticomuscular coherence during dynamic force output. Neuroimage 34(3):1191–1198

Patino L, Omlor W, Chakarov V, Hepp-Reymond MC, Kristeva R (2008) Absence of gamma-range corticomuscular coherence during dynamic force in a deafferented patient. J Neurophysiol 99(4):1906–1916

Perret C, Cabelguen JM (1980) Main characteristics of the hindlimb locomotor cycle in the decorticate cat with special reference to bifunctional muscles. Brain Res 187(2):333–352

Petersen TH, Willerslev-Olsen M, Conway BA, Nielsen JB (2012) The motor cortex drives the muscles during walking in human subjects. J Physiol 590(10):2443–2452

Poston B, Danna-Dos Santos A, Jesunathadas M, Hamm TM, Santello M (2010) Force-independent distribution of correlated neural inputs to hand muscles during three-digit grasping. J Neurophysiol 104:1141–1154

Salenius S, Hari R (2003) Synchronous cortical oscillatory activity during motor action. Curr Opin Neurobiol 13(6):678–684

Salenius S, Portin K, Kajola M, Salmelin R, Hari R (1997) Cortical control of human motoneuron firing during isometric contraction. J Neurophysiol 77(6):3401–3405

Schoffelen JM, Oostenveld R, Fries P (2005) Neuronal coherence as a mechanism of effective corticospinal interaction. Science 308(5718):111–113

Scholz JP, Schöner G (1999) The uncontrolled manifold concept: identifying control variables for a functional task. Exp Brain Res 126(3):289–306

Semmler JG, Ebert SA, Amarasena J (2013) Eccentric muscle damage increases intermuscular coherence during a fatiguing isometric contraction. Acta Physiol 208(4):362–375

Severini G, Conforto S, Schmid M, D'Alessio T (2012) A multivariate auto-regressive method to estimate cortico-muscular coherence

for the detection of movement intent. Appl Bionics Biomech 9(2):135–143

Smith JC, Abdala AP, Borgmann A, Rybak IA, Paton JF (2013) Brainstem respiratory networks: building blocks and microcircuits. Trends Neurosci 36(3):152–162

Terry K, Griffin L (2008) How computational technique and spike train properties affect coherence detection. J Neurosci Methods 168(1):212–223

Welch PD (1967) The use of fast Fourier transform for the estimation of power spectra: a method based on time averaging over short, modified periodograms. IEEE Trans Audio Electroacoust 15(2):70–73

Zhong G, Shevtsova NA, Rybak IA, Harris-Warrick RM (2012) Neuronal activity in the isolated mouse spinal cord during spontaneous deletions in fictive locomotion: insights into locomotor central pattern generator organization. J Physiol 590(19):4735–4759